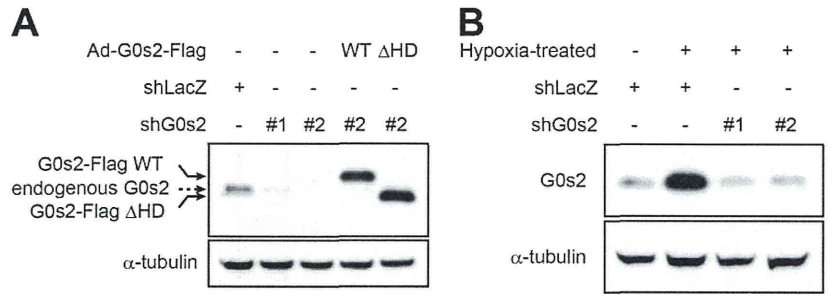

Fig. S7. (*A*) Immunoblotting of G0s2-depleted cardiomyocytes rescued by overexpression of G0s2-Flag. (*B*) Immunoblotting of G0s2-depleted cardiomyocytes under hypoxic conditions. Cardiomyocytes expressing the indicated adenovirus were exposed to hypoxia (1% O_2) for 4 h. The cell lysates were subjected to immunoblotting with anti-G0s2 or α-tubulin antibodies.

Table S1. The identification of proteins that specifically bound to G0s2 by MS

SwissProt accession	Description	Molecular mass (Da)	PLGS score	Peptides	Coverage (%)
ATPA_RAT	ATP synthase subunit-α mitochondrial	59,716	10.5798	10	18.9873
ATPB_RAT	ATP synthase subunit-β mitochondrial	56,318	10.5798	11	24.1966
ATPG_RAT	ATP synthase γ-chain	32,975	10.523	2	7.3826
ATP5F1_RAT	ATP synthase subunit b mitochondrial	28,850	10.5796	2	3.9063
ATPO_RAT	ATP synthase subunit O mitochondrial	23,382	10.5796	5	23.9437
ATP5H_RAT	ATP synthase subunit d mitochondrial	18,751	10.5796	2	13.0435
ATPD_RAT	ATP synthase subunit-δ mitochondrial	17,584	10.5796	2	13.6905
D3ZAF6_RAT	ATP synthase H transporting mitochondrial Fo complex subunit f isoform 2	10,972	10.5796	2	22.3404

A PLGS score was calculated by the Protein Lynx Global Server (PLGS; PLGS 2.4) software using a Monte Carlo algorithm to analyze all of the available MS data; this score is a statistical measure of the accuracy of assignation. A higher score implies a greater confidence in the identity of the protein.

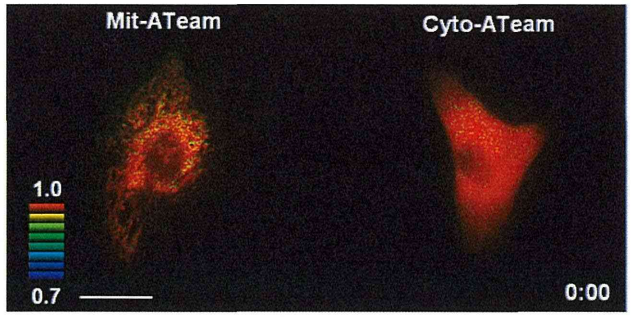

Movie S1. Time-lapse imaging of the (*Left*) Mit-ATeam and (*Right*) Cyto-ATeam fluorescence in cardiomyocytes before and after the addition of oxidative phosphorylation inhibitor. YFP/CFP ratiometric pseudocolored images were obtained every 1 min for 25 min. Oligomycin A (0.01 μg/mL), an inhibitor of F_oF_1-ATP synthase, was added at time point 5 min. (Scale bar: 20 μm.)

Movie S1

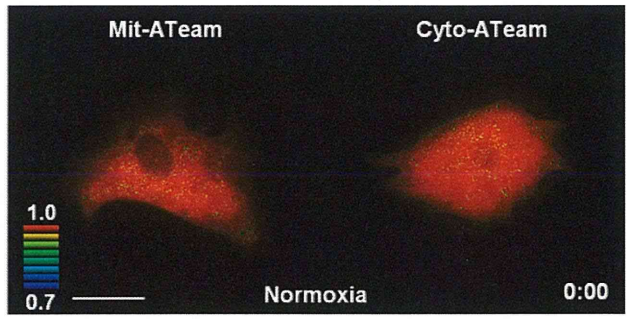

Movie S2. Time-lapse imaging of the (*Left*) Mit-ATeam and (*Right*) Cyto-ATeam fluorescence in cardiomyocytes exposed to hypoxia. YFP/CFP ratiometric pseudocolored images were obtained every 30 min for 3 h. Cells are exposed to 1% hypoxia from the time point 30 min. (Scale bar: 20 μm.)

Movie S2

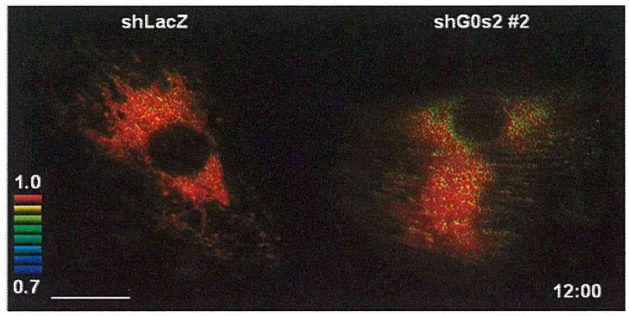

Movie S3. Time-lapse imaging of the Mit-ATeam fluorescence in cardiomyocytes that expressed (*Left*) shLacZ or (*Right*) shG0s2 #2. YFP/CFP ratiometric pseudocolored images were obtained every 1 h for 12 h. An inhibitor of F_oF_1-ATP synthase (1 μg/mL oligomycin A) was added at the end of time-lapse imaging to completely inhibit ATP synthesis. (Scale bar: 20 μm.) The indicated times designate the periods after adenovirus infection.

Movie S3

Movie S4. Time-lapse imaging of the Cyto-ATeam fluorescence in cardiomyocytes that expressed (*Left*) shLacZ or (*Right*) shG0s2 #2. YFP/CFP ratiometric pseudocolored images were obtained every 1 h for 12 h. Inhibitors of both glycolysis (10 mM 2-deoxyglucose) and F_oF_1-ATP synthase (1 μg/mL oligomycin A) were added at the end of the time-lapse imaging to decrease the cytosolic ATP concentration. (Scale bar: 20 μm.) The indicated times designate the periods after adenovirus infection.

Movie S4

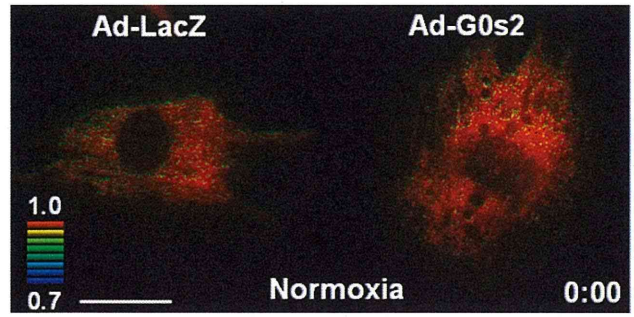

Movie S5. Time-lapse imaging of the Mit-ATeam fluorescence in cardiomyocytes that expressed (*Left*) LacZ or (*Right*) G0s2 during hypoxia and reoxygenation. YFP/CFP ratiometric pseudocolored images were obtained every 30 min for 4 h. The cells were exposed and imaged under hypoxic condition from the time point 30 min to 4 h. (Scale bar: 20 μm.)

Movie S5

International Journal of Cardiology 172 (2014) e288–e289

Contents lists available at ScienceDirect

International Journal of Cardiology

journal homepage: www.elsevier.com/locate/ijcard

Letter to the Editor

Comprehensive metagenomic approach for detecting causative microorganisms in culture-negative infective endocarditis

Atsuko Imai [a], Kazuyoshi Gotoh [b], Yoshihiro Asano [a,*], Noriaki Yamada [a], Daisuke Motooka [b], Masaki Fukushima [a], Machiko Kanzaki [a], Tomohito Ohtani [a], Yasushi Sakata [a], Hiroyuki Nishi [c], Koichi Toda [c], Yoshiki Sawa [c], Issei Komuro [a], Toshihiro Horii [b], Tetsuya Iida [b], Shota Nakamura [b], Seiji Takashima [a,d]

[a] Department of Cardiovascular Medicine, Osaka University Graduate School of Medicine, Suita, Osaka, Japan
[b] Department of Infection Metagenomics, Research Institute for Microbial Diseases, Osaka University, Suita, Osaka, Japan.
[c] Department of Cardiovascular Surgery, Osaka University Graduate School of Medicine, Suita, Osaka, Japan
[d] Department of Medical Biochemistry, Osaka University Graduate School of Medicine, Suita, Osaka, Japan

ARTICLE INFO

Article history:
Received 14 November 2013
Accepted 28 December 2013
Available online 8 January 2014

Keywords:
Metagenomic analysis
Culture-negative infective endocarditis
Next generation sequencing

A recent nationwide survey of infective endocarditis (IE) showed that IE is still a lethal disease, with an in-hospital death rate of 11% [1]. Detecting causative microorganisms plays an important role in choosing optimal antibiotics and effective dosing periods [2]. However, culture-negative IE was frequently observed, especially among cases that included premedication with antimicrobial agents [3]. Previous studies reported that valve culture has low sensitivity between 8% and 13% [4,5]. Furthermore, valve culture can detect only viable and target microorganisms with the culture medium currently available. Recently, the metagenomic approach using Next Generation Sequencing (NGS) emerged as a comprehensive method for exploring causative agents of infectious diseases without prior culture [6]. Therefore, we assessed the viability of metagenomic approach to detect causative microorganisms in resected valves from IE patients.

We conducted metagenomic analyses using NGS technology for resected valves in 3 IE cases. Between May 2012 and February 2013, 3 IE patients who had been admitted to the cardiovascular department at Osaka University, Suita, Japan, underwent metagenomic analyses of resected valves. Case 1 is a 55-year-old female with IE of the native aortic valve. Case 2 is a 57-year-old male who presented with IE of both native aortic and mitral valves. Case 3 is a 74-year-old female with IE of the native aortic valve.

We extracted DNA from the homogenized valve using the QIAamp cador Pathogen Mini kit (QIAGEN). Using the Nextera DNA sample preparation kit (Illumina), a sequencing library was prepared from the extracted DNA. We then performed metagenomic shotgun sequencing on the MiSeq platform (Illumina) according to the manufacturer's protocol. Obtained reads were trimmed of low-quality sequences and subjected to the NCBI BLAST search against the Genbank nt database. We assigned taxonomy based on the NCBI taxonomy database.

In 2 culture-positive cases, metagenomic results of resected valves were consistent with cultivation results. In case 1, the blood culture at the primary hospital was positive for *Enterococcus faecalis* after administration of several antibiotics and negative at the time of referral to our hospital. The resected valve culture was also positive for *E. faecalis*. In case 2, both the blood and valve cultures were positive for *Streptococcus mutans* without any prior administration of antibiotics. The results of metagenomic sequencing of resected aortic valves were summarized in Table 1. In both cases, the dominant parts in bacteria-derived sequences could be mapped on the genomes of candidate bacterial species using BLAST search, *E. faecalis* and *S. mutans* respectively

Table 1
Summary of the sequencing results of resected aortic valves.

	Case 1		Case 2*		Case 3	
	no.	(%)	no.	(%)	no.	(%)
Total reads	327,913	100.0	322,497	100.0	425,706	100.0
Reads from human genome	314,507	95.9	319,257	99.0	410,300	96.4
Reads from bacterial genome						
	E. faecalis (NC_019770)		S. mutans (NC_013928)		S. sanguinis (NC_009009)	
	2251	0.68	145	0.047	72	0.017

* Metagenomic analysis of resected mitral valve also detected *Streptococcus mutans*.

* Corresponding author at: Department of Cardiovascular Medicine, Osaka University Graduate School of Medicine, 2-2 Yamadaoka, Suita, Osaka 565-0871, Japan. Tel.: +81 6 6879 3492; fax: +81 6 6879 3493.
E-mail address: asano@cardiology.med.osaka-u.ac.jp (Y. Asano).

http://dx.doi.org/10.1016/j.ijcard.2013.12.197

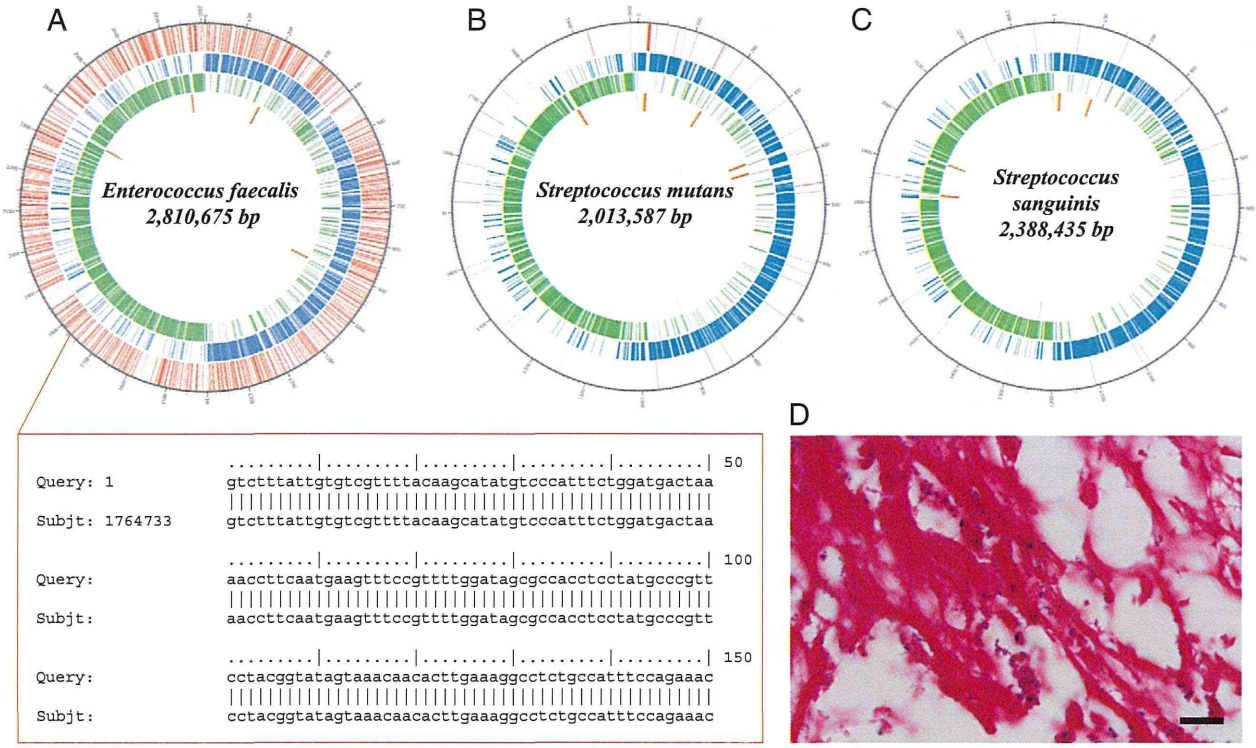

Fig. 1. (A–C) Circular genome maps of target bacteria. Outer layer shows fragments detected in each analysis (Red), the second outer layer, positive strand genes of target bacteria (Blue); the third outer layer, negative strand genes of target bacteria (Green); the fourth outer layer, ribosomal/transfer RNA of target bacteria (Orange). Reference genome maps of *Enterococcus faecalis* for case 1 (A), *Streptococcus mutans* for case 2 (B), and *Streptococcus sanguinis* for case 3 (C), respectively. Representative sequences detected by NGS technology was shown in A. (D) Gram-staining of the resected valve tissue in case 3 Gram-positive cocci were identified indicated. Scale bar;10 μM.

(Fig. 1A, B). Metagenomic results were consistent with culture results in both cases.

Besides culture positive cases, the metagenomic approach could also detect causative organism of IE in 1 culture-negative case. In case 3, both the blood and valve cultures were negative at our hospital after the patient took several antibiotics prior to admission. Genome mapping using metagenomic data showed *Streptococcus sanguinis* as a causative bacterium (Fig. 1C). It was confirmed by Gram-staining, in which Gram-positive cocci were identified in the valve tissue (Fig. 1D).

To our knowledge, this is the first report to successfully identify bacterial genome fragments using NGS and to show the superiority of this approach over valve culture in detecting microorganisms in culture-negative IE.

In general, there are three major advantages of NGS metagenomic analysis in detecting causative microorganisms of IE compared to conventional methods. First, metagenomic shotgun sequencing by NGS can screen for various microorganisms, including viruses and fungi, whereas targeted amplicon sequencing such as 16S rRNA sequencing can only screen for bacteria [7]. Second, metagenomic NGS analysis can detect nonviable or unculturable microorganisms as long as microbial nucleic acids remain in the specimen, which overcomes the limitation of low sensitivity in conventional culture-based methods. Thirdly, unlike the 16S rRNA analysis, it can yield high-throughput sequence reads covering genome-wide regions, which has a potential to be used for multi-locus sequence typing analysis [8]. All these advantages indicate promising clinical application of this method.

Although studies with larger samples are required to confirm the validity of our initial results, our results showed the possibility metagenomic shotgun sequencing by NGS can be added to current screening methods for detecting microorganisms, especially in culture-negative IE.

The authors of this manuscript have certified that they comply with the Principles of Ethical Publishing in the International Journal of Cardiology.

References

[1] Nakatani S, Mitsutake K, Ohara T, et al. Recent picture of infective endocarditis in Japan. Circ J Mar 23 2013;77(6):1158–64.
[2] Habib G, Hoen B, Tornos P, et al. ESC Committee for Practice Guidelines. Guidelines on the prevention, diagnosis, and treatment of infective endocarditis (new version 2009). Eur Heart J 2009;30:2369–413.
[3] Mylonakis E, Calderwood SB. Infective endocarditis in adults. N Engl J Med 2001;345:1318–30.
[4] Greub G, Lepidi H, Rovery C, et al. Diagnosis of infectious endocarditis in patients undergoing valve surgery. Am J Med 2005;118:230–8.
[5] Breitkopf C, Hammel D, Scheld HH, Peters G, Becker K. Impact of a molecular approach to improve the microbiological diagnosis of infective heart valve endocarditis. Circulation 2005;111:1415–21.
[6] Capobianchi MR, Giombini E, Rozera G. Next-generation sequencing technology in clinical virology. Clin Microbiol Infect 2013;19:15–22.
[7] Shah N, Tang H, Doak TG, Ye Y. Comparing bacterial communities inferred from16S rRNA gene sequencing and shotgun metagenomics. Pac Symp Biocomput 2011:165–1176.
[8] Do T, Gilbert SC, Klein J, Warren S, Wade WG, Beighton D. Clonal structure of *Streptococcus sanguinis* strains isolated from endocarditis cases and the oral cavity. Mol Oral Microbiol 2011;26:291–302.

frontiers in
GENETICS

ORIGINAL RESEARCH ARTICLE
published: 05 December 2013
doi: 10.3389/fgene.2013.00271

Aberrantly methylated genes in human papillary thyroid cancer and their association with *BRAF/RAS* mutation

Yasuko Kikuchi[1,2], Eiichi Tsuji[2], Koichi Yagi[1], Keisuke Matsusaka[3], Shingo Tsuji[1], Junichi Kurebayashi[4], Toshihisa Ogawa[2], Hiroyuki Aburatani[1] and Atsushi Kaneda[1,5,6]*

[1] *Genome Science Division, Research Center for Advanced Science and Technology, The University of Tokyo, Tokyo, Japan*
[2] *Department of Metabolic Care and Endocrine Surgery, Graduate School of Medicine, The University of Tokyo, Tokyo, Japan*
[3] *Department of Pathology, Graduate School of Medicine, The University of Tokyo, Tokyo, Japan*
[4] *Department of Breast and Endocrine Surgery, Kawasaki Medical University, Okayama, Japan*
[5] *Department of Molecular Oncology, Graduate School of Medicine, Chiba University, Chiba, Japan*
[6] *CREST, Japan Science and Technology Agency, Saitama, Japan*

Edited by:
Yoshimasa Saito, Keio University Faculty of Pharmacy, Japan

Reviewed by:
Craig A. Cooney, Central Arkansas Veterans Healthcare System, USA
Michèle Amouyal, Centre National de la Recherche Scientifique, France

***Correspondence:**
Atsushi Kaneda, Department of Molecular Oncology, Graduate School of Medicine, Chiba University, Inohana 1-8-1, Chuo-ku, Chiba-City 260-8670, Japan
e-mail: kaneda@chiba-u.jp

Cancer arises through accumulation of epigenetic and genetic alteration. Aberrant promoter methylation is a common epigenetic mechanism of gene silencing in cancer cells. We here performed genome-wide analysis of DNA methylation of promoter regions by Infinium HumanMethylation27 BeadChip, using 14 clinical papillary thyroid cancer samples and 10 normal thyroid samples. Among the 14 papillary cancer cases, 11 showed frequent aberrant methylation, but the other three cases showed no aberrant methylation at all. Distribution of the hypermethylation among cancer samples was non-random, which implied existence of a subset of preferentially methylated papillary thyroid cancer. Among 25 frequently methylated genes, methylation status of six genes (*HIST1H3J, POU4F2, SHOX2, PHKG2, TLX3, HOXA7*) was validated quantitatively by pyrosequencing. Epigenetic silencing of these genes in methylated papillary thyroid cancer cell lines was confirmed by gene re-expression following treatment with 5-aza-2′-deoxycytidine and trichostatin A, and detected by real-time RT-PCR. Methylation of these six genes was validated by analysis of additional 20 papillary thyroid cancer and 10 normal samples. Among the 34 cancer samples in total, 26 cancer samples with preferential methylation were significantly associated with mutation of *BRAF/RAS* oncogene ($P = 0.04$, Fisher's exact test). Thus, we identified new genes with frequent epigenetic hypermethylation in papillary thyroid cancer, two subsets of either preferentially methylated or hardly methylated papillary thyroid cancer, with a concomitant occurrence of oncogene mutation and gene methylation. These hypermethylated genes may constitute potential biomarkers for papillary thyroid cancer.

Keywords: DNA methylation, thyroid cancer, CIMP (CpG island methylator phenotype), BRAF, RAS, oncogene mutation

INTRODUCTION

Papillary thyroid cancer is the most common cancer derived from follicular cells. It is estimated that approximately 23,500 cases of differentiated thyroid cancer occur per year in the United States (Jemal et al., 2005), and 19,000 papillary thyroid cancer cases per year in the European Union (http://globocan.iarc.fr/). In Japan, about 8000 patients suffer from thyroid cancer every year, 80% of which are papillary cancer. While prognosis for papillary thyroid cancer is generally good, with a 10-year survival rate above 90%, some patients die of distant metastases and/or repeated recurrence (Ezaki et al., 1992; Yamashita et al., 1998).

RET/PTC (Rearranged in Transformation/Papillary Thyroid Carcinoma) re-arrangement, *BRAF* (V-Raf murine sarcoma viral oncogene homolog B) and *RAS* (Rat Sarcoma viral oncogene homolog) point mutations are frequently observed in papillary thyroid cancer (Mitsutake et al., 2006; Knauf and Fagin, 2009). Mutation of T to A at 1799 in the exon 15 of the *BRAF* gene has been reported in 28–69% of papillary thyroid cancer cases, while point mutations of *RAS* genes are detected in 5–20% (Cohen et al., 2003; Kimura et al., 2003; Namba et al., 2003; Kondo et al., 2007). Papillary thyroid cancer with poor prognosis is associated with *BRAF* mutation (Xing et al., 2005; Lee et al., 2012), whereas concomitantly, lengthy disease-free interval is not (Ulisse et al., 2012).

Patients with papillary thyroid cancer are generally treated by surgery. But it is difficult to decide whether total thyroidectomy, hemithyroidectomy, prophylactic central neck dissection or no dissection, should be performed in patients without preoperative or intraoperative evidence of metastatic lymph nodes (Xing et al., 2013). Association of *BRAF* mutation with occult central neck lymph node metastases (Joo et al., 2012) might support use of *BRAF* mutation as an indication for prophylactic central neck dissection for patients with conventionally low- to intermediate-risk papillary thyroid cancer. But precise diagnosis to define prognosis and suitable therapy is currently impossible. Molecular biomarkers would therefore simplify disease management (McLeod et al., 2013).

Along with genetic alterations, accumulation of epigenetic alterations is known to affect cancer development (Baylin and Ohm, 2006; Feinberg et al., 2006; Esteller, 2007). Aberrant DNA methylation at promoter regions is a major epigenetic alteration to silence tumor suppressor genes in many cancer types. *RASSF1A* (Ras association (RalGDS/AF-6) domain family member 1) is methylated in 20% of papillary thyroid cancer, leading to activation of the RAS-MAPK (Mitogen-Activated Protein Kinase) signal (Xing et al., 2004). Papillary thyroid cancer is also reported to involve methylation of other genes, including *RARB* (Retinoic Acid Receptor, Beta), $p16^{INK4A}$ (*CDKN2A*, Cyclin-Dependent Kinase Inhibitor 2A), *TSHR* (Thyroid Stimulating Hormone Receptor), *CDH1* (Cadherin 1, type 1, E-cadherin), *DAPK* (Death-Associated Protein Kinase 1), and *MLH1* (mutL Homolog 1) (Hoque et al., 2005; Guan et al., 2008; Mohammadi-asl et al., 2011). While a few genes known to be aberrantly methylated in other cancers were analyzed in these studies, methylation frequencies ranged from 15 to 33%. Involvement of genes in aberrant DNA methylation, however, has not been well-clarified in papillary thyroid cancer. Whether any subset of papillary thyroid cancer shows preferential aberrant methylation, and whether such methylation and other clinicopathological factors are associated are also unclear.

We here analyzed DNA methylation status of promoter regions on a genome-wide scale, using the Illumina Infinium HumanMethylation27 BeadChip technique on 14 clinical papillary thyroid cancer samples and 10 normal thyroid samples. For genes frequently hypermethylated in cancer, methylation status was validated quantitatively by pyrosequencing, using 20 additional clinical cancer samples and 10 additional normal samples. Methylation-associated gene silencing was confirmed by gene re-expression following 5-aza-2′-deoxycytidine and trichostatin A treatment, and by quantitative reverse transcription-polymerase chain reaction (RT-PCR) on thyroid cancer cell lines. We found a number of genes with frequent aberrant methylation and silencing in papillary thyroid cancer, and a subset of cancer with preferential aberrant methylation.

MATERIALS AND METHODS

CLINICAL SAMPLES AND CELL LINES

We obtained 79 primary papillary thyroid cancer samples from patients who underwent thyroidectomy at The University of Tokyo, with written informed consent. These samples were immediately frozen with liquid nitrogen and stored at −80°C. The frozen materials were microscopically examined for cancer cell contents by pathologists and were dissected to enrich cancer cells when necessary. Thirty-four cancer samples containing more than 40% of cancer cells were selected and used for further analysis. DNA was extracted by QIAamp DNA Micro Kit (QIAGEN, Valencia, CA). Thyroid cancer cell line BHT-101 was obtained from DSMZ (Leibniz Institute DSMZ-German Collection of Microorganisms and Cell Cultures), TPC-1 was provided from Dr. Mitsutake, University of Nagasaki (Ishizaka et al., 1989) and KTC-1 and KTC-3 cell lines were provided from Dr. Kurebayashi, Kawasaki Medical University (Kurebayashi et al., 2000, 2006). These cell lines were maintained in RPMI 1640 (Gibco, Grand Island, NY) supplemented with 10% fetal bovine serum, streptomycin sulfate (100 mg/L), and penicillin G sodium (100 mg/L). Peripheral blood cell samples were purchased from The Coriell Cell Repositories. This research was certified by the Ethics Committee of The University of Tokyo and Chiba University.

INFINIUM ASSAYS

High-resolution methylation analysis was conducted on the Illumina Infinium HumanMethylation27 microarray platform. This BeadChip assay measures methylation, given as a β-value, at more than 27,000 CpG loci covering 15,000 genes. For each CpG site, the β-value is the ratio of the fluorescence signal from the methylated probe over the sum of methylated and unmethylated probe signals. The β-value, ranging from 0.00 to 1.00, reflects the methylation level of the individual CpG site. Bisulfite conversion, whole-genome amplification, labeling, hybridization, and scanning were carried out according to the manufacturer's protocols. According to the previously proposed classification (Weber et al., 2007), Infinium probes were classified into three categories: high-CpG, intermediate-CpG, and low-CpG probes, on the basis of CpG ratio (the ratio of observed CpG count over expected CpG count) and GC contents within 500 bp region around the probe site (Matsusaka et al., 2011). Genes in X and Y chromosomes were excluded to avoid gender differences. Infinium enables us to analyze DNA methylation levels systematically for more than 14,000 genes, but methylation level of a single CpG site detected by Infinium may not precisely represent methylation status of promoter CpG island. Some Infinium probes might be less quantitative; in analysis of control samples with known levels of methylation (0, 25, 50, 75, 100%), the observed β-values generally correlated with the expected β-values, while some probes showed lower β-values (0.0–0.3) for 75% control or higher β-values (0.7–1.0) for 25% control (Nagae et al., 2011).

PYROSEQUENCING ANALYSIS

Quantitative validation for methylation status was carried out by pyrosequencing as previously reported (Matsusaka et al., 2011). Primers were designed to include no or only one CpG site in a primer sequence using Pyro Q-CpG Software (QIAGEN), to amplify bisulfite-treated DNA regions containing several CpG sites. For C of CpG site within a primer sequence, a nucleotide which does not anneal to C or U was chosen, e.g., adenosine (A). Briefly, the biotinylated PCR product was bound to streptavidin sepharose beads HP (Amersham Biosciences, Sweden), washed, and denatured using a 0.2 mol/L NaOH solution. After addition of 0.3 μmol/L sequencing primer to the purified, single-stranded PCR product, pyrosequencing was carried out using PyroMark Q96 ID System (QIAGEN) according to the manufacturer's instructions. Primer sequences and conditions for *HIST1H3J* (Histone cluster 1, H3j), *POU4F2* (POU class 4 homeobox 2), *SHOX2* (Short stature homeobox 2), *PHKG2* (Phosphorylase Kinase, Gamma 2), *TLX3* (T-cell Leukemia homeobox 3), and *HOXA7* (Homeobox A7), are shown in **Table 1**. Control samples with known levels of methylation (0, 25, 50, 75, 100%) were prepared as previously described (Yagi et al., 2010). Pyrosequencing is not systematic, but highly quantitative (Matsusaka et al., 2011), and enables us to precisely validate the methylation level at one

Table 1 | Primer sequences for pyrosequencing of six potential methylation biomarkers.

Genes	Primer sequences for PCR (Forward/Reverse)		Sequencing primers
HIST1H3J	F	GTTATAAATTTTGGTAGAAGTTATTGT	ATGGTTAGGAAGAAGTAGATAGT
	R*	ACCTTAATAACCAACTACTTCC	
POU4F2	F	GGGGAGAGGGGAGTATAA	ATTAGTTTAGATTGATAGTAGAGG
	R*	AAAAAAAACTATACCAAATTAAACTCACCC	
SHOX2	F*	TTGGGGGGGTTGGAGTAGTAAA	AACCCCCTAAATTCTTCCAT
	R	CTCCTTCTTCTCCTTCACTTTCTAATC	
PHKG2	F	GTTTGTAATTTTAGTATTTTGGGAGGTTGA	AAGTTTAAGGTTGTAGTGA
	R*	TCCCTAACTAAATTCAACATTTTCTCTT	
TLX3	F	TGGTTGAGGTAGGAGAGGAATTAGTA	GGTTTAAGAAAGATGATATAGAG
	R*	CACTAAAACTTTACCAAAAATAC	
HOXA7	F*	GGGAGTAAAGGAGTAAGAAGT	CAACAAATCACAAATCAAAATTA
	R	ACCCAACAACAAATCACAAATCAAAATT	

**Primers with 5′-biotin tag.*

CpG site, as determined by the Infinium assay, as well as at surrounding CpG sites. Mean methylation levels of these CpG sites were calculated to represent methylation status of each gene promoter, and were displayed in figures by heatmap or dot chart.

Mutation analysis

Mutations at *BRAF* 1799, *KRAS* (Kirsten Rat Sarcoma viral oncogene homolog) 34, 35, 38, *NRAS* (Neuroblastoma RAS viral oncogene homolog) 181, 182, 183, *HRAS* (Harvey Rat Sarcoma viral oncogene homolog) 35, 37, 181, 182, 183, were analyzed by genotyping assays on MassARRAY platform, by detecting mass difference of the extended nucleotide using matrix assisted laser desorption ionization-time of flight-mass spectrometry (MALDI-TOF-MS) (Yagi et al., 2012). First, PCR amplification primers and a post-PCR extension primer were designed using MassARRAY Assay Design 3.0 software (Sequenom), and listed in **Table 2**. Those mutations were analyzed in a single reaction by multiplex PCR. PCR amplification was performed in 5-μL volume containing 0.5 unit of Taq polymerase, 5 ng of genomic DNA, 0.5 pmol of PCR primer and 2.5 nmol of dNTPs. PCR reactions were cycled at 94°C for 15 min, followed by 45 cycles of 94°C for 20 s, 56°C for 30 s and 72°C for 1 min. Shrimp alkaline phosphatase treatment was performed at 37°C for 20 min and 85°C for 5 min. Post-PCR primer extension was carried out using 5.6 pmol of extension primer. Extension reaction was cycled at 94°C for 30 s, followed by 40 cycles of 94°C for 5 s, 5 cycles of 52°C for 5 s and 80°C for 5 s, and 72°C for 3 min. Reaction products were transferred to a SpectroCHIP (Sequenom) and mass difference was analyzed using MALDI-TOF-MS. Irradiation of the matrix-oligonucleotide-cocrystal with a laser beam ultimately results in desorption and ionization of the oligonucleotides, which then can be accelerated in an electrical field into the TOF device. The TOF device separates the accelerated analyte ions of different mass-to-charge (m/z) ratios by providing a field-free drift tube of defined length. After passing through the tube, ions are detected; every signal is assigned to a specific molecular mass calculated from the TOF. The extended bases at possible mutation sites are determined from the difference of nucleotide molecular masses (Vogel et al., 2009).

5-Aza-2′-DEOXYCYTIDINE AND TRICHOSTATIN A TREATMENT

Thyroid cancer cell lines were cultured at a density of 3×10^5 cells/10-cm dish on Day 0. Cells were exposed to 3 μM 5-aza-2′-deoxycytidine (Sigma-Aldrich, St. Louis, MO) on Days 1, 2, and 3, and to 300 nM trichostatin A (Sigma-Aldrich) on the Day 3. 5-Aza-2′-deoxycytidine induces hypomethylation of DNA by inhibiting DNA methyltransferase, and re-expression of silenced genes by 5-aza-2′-deoxycytidine treatment is synergistically enhanced by trichostatin A, a histone deacetylase inhibitor (Suzuki et al., 2002). 5-Aza-2′-deoxycytidine is unstable in aqueous solution, and thus a 20 mM solution in dimethyl sulfoxide (DMSO) was freshly prepared, and diluted in medium to 3 μM every day immediately before medium change. The medium was changed every 24 h, and the cells were harvested on Day 4.

QUANTITATIVE PCR ANALYSIS

RT-PCR was performed using CFX96 Touch TM Real-Time PCR Detection System (BIORAD Laboratories). cDNA was synthesized from 1 μg of total RNA treated with DNase I with a Superscript III kit (Invitrogen, Life Technologies). The quantity of cDNA of each gene in a sample was measured by comparing it with standard samples that contained 10^1 to 10^6 copies of the genes, and normalized to that of *PPIA* (Peptidylprolyl Isomerase A). Primer sequences are shown in **Table 3**.

STATISTICAL ANALYSIS

P-values were calculated to compare methylation(+) cancer and methylation(−) cancer and to analyze the correlation of the methylation status to clinicopathological features. Fisher's exact test was used for analysis of binary features such as sex, distant metastasis, recurrence, and mutation of *BRAF*/*RAS* oncogenes (with simple choice between male and female, occurrence and no occurrence); *t*-test was used for more descriptive features that do not imply a choice, such as age, tumor size, number of lymph nodes with metastasis, and thyroglobulin. When $P < 0.05$, the correlation was considered statistically significant. *P*-values were also calculated by *t*-test to compare distribution of methylation

Table 2 | Primer sequences used for mutation analysis (MALDI-TOF-MS assays).

Mutation sites	Primer sequences (Forward/Reverse)		Extend primers
BRAF_1799	F	ACGTTGGATGTTCAAACTGATGGGACCCAC	TGATTTTGGTCTAGCTACAG
	R	ACGTTGGATGTCTTCATGAAGACCTCACAG	
HRAS_34	F	ACGTTGGATGAATGGTTCTGGATCAGCTGG	ACTCTTGCCCACACCGC
	R	ACGTTGGATGGACGGAATATAAGCTGGTGG	
HRAS_35	F	ACGTTGGATGAATGGTTCTGGATCAGCTGG	AGCGGGTGGTGGTGGGCGCCG
	R	ACGTTGGATGGACGGAATATAAGCTGGTGG	
HRAS_37	F	ACGTTGGATGAATGGTTCTGGATCAGCTGG	TCATCGCACTCTTGCCCACAC
	R	ACGTTGGATGGACGGAATATAAGCTGGTGG	
HRAS_38	F	ACGTTGGATGAATGGTTCTGGATCAGCTGG	CAGCGCACTCTTGCCCACA
	R	ACGTTGGATGGACGGAATATAAGCTGGTGG	
HRAS_181	F	ACGTTGGATGTGGCAAACACACACAGGAAG	CATGGCGCTGTACTCCTCCT
	R	ACGTTGGATGTGTTGGACATCCTGGATACC	
HRAS_182	F	ACGTTGGATGTGGCAAACACACACAGGAAG	CATGGCGCTGTACTCCTCC
	R	ACGTTGGATGTGTTGGACATCCTGGATACC	
HRAS_183	F	ACGTTGGATGTGGCAAACACACACAGGAAG	CGCATGGCGCTGTACTCCTC
	R	ACGTTGGATGTGTTGGACATCCTGGATACC	
KRAS_34	F	ACGTTGGATGTAGCTGTATCGTCAAGGCAC	ACTCTTGCCTACGCCAC
	R	ACGTTGGATGAGGCCTGCTGAAAATGACTG	
KRAS_35	F	ACGTTGGATGTAGCTGTATCGTCAAGGCAC	CTGTGGTAGTTGGAGCTG
	R	ACGTTGGATGAGGCCTGCTGAAAATGACTG	
KRAS_37	F	ACGTTGGATGTAGCTGTATCGTCAAGGCAC	GAGGGGCACTCTTGCCTACGC
	R	ACGTTGGATGAGGCCTGCTGAAAATGACTG	
KRAS_38	F	ACGTTGGATGTAGCTGTATCGTCAAGGCAC	AGGCACTCTTGCCTACG
	R	ACGTTGGATGAGGCCTGCTGAAAATGACTG	
NRAS_181	F	ACGTTGGATGTCGCCTGTCCTCATGTATTG	ATACTGGATACAGCTGGA
	R	ACGTTGGATGCCTGTTTGTTGGACATACTG	
NRAS_182	F	ACGTTGGATGTCGCCTGTCCTCATGTATTG	ATGGCACTGTACTCTTCT
	R	ACGTTGGATGCCTGTTTGTTGGACATACTG	
NRAS_183	F	ACGTTGGATGTCGCCTGTCCTCATGTATTG	CTGGATACAGCTGGACA
	R	ACGTTGGATGCCTGTTTGTTGGACATACTG	

Table 3 | Primer sequences for real-time RT-PCR in gene re-expression analysis.

Gene	Primer sequences (Forward/Reverse)		Anneal (°C)	Product (bp)
HIST1H3J	F	AAATCAAGCAGAGGCGAAGTCGGA	58	106
	R	GGATAGTGGGTCTCGTCAAAAAGC		
POU4F2	F	CACCAAGCCTGAACTCTTCAAT	58	101
	R	GCTGAATGGCAAAGTAGGCTTCG		
SHOX2	F	AAATCAAGCAGAGGCGAAGTCGGA	58	85
	R	GGATAGTGGGTCTCGTCAAAAAGC		
PHKG2	F	TGATCTTGTTCACACTCCTGGCT	58	145
	R	GAGATCAGGTCTTTGACAGTGCT		
TLX3	F	CTGTCTGCACAACTCGTCACTCTT	60	79
	R	GACAGCGGGAACCTTGGAACTATC		
HOXA7	F	AGTTCCACTTCAACCGCTACCTGAC	58	131
	R	GTCCTTATGCTCTTTCTTCCACTTC		

ratios between cancer and normal samples. When $P < 0.05$, the difference of the methylation ratios between cancer and normal samples was considered statistically significant. The dot chart and heatmap were drawn using Excel software and Java TreeView software (http://jtreeview.sourceforge.net/).

RESULTS

ONCOGENE MUTATION STATUS IN PAPILLARY THYROID CANCER

We analyzed mutation status of *BRAF* and *RAS* (*HRAS*, *NRAS*, and *KRAS*) oncogenes in 34 papillary thyroid cancer samples using MALDI-TOF-MS (**Figure 1**). *BRAF* mutation was detected

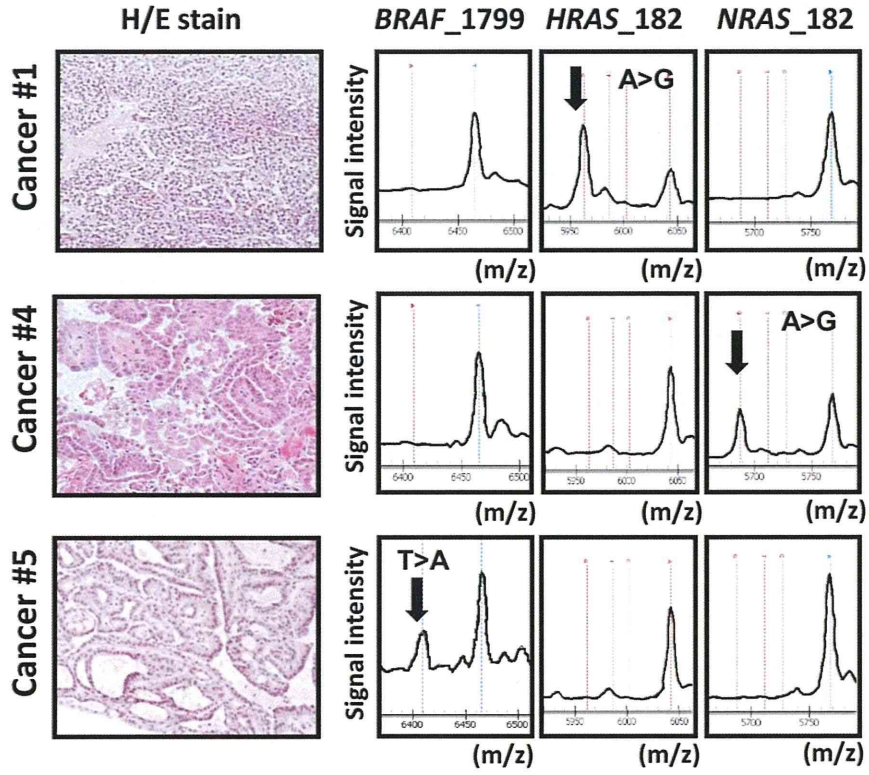

FIGURE 1 | Representative data obtained from MALDI-TOF-MS imaging for three cancer samples. Cancer samples #1, #4, and #5 correspond to papillary cancer samples #1, #4, and #5 in **Figure 3**. First column: photomicrograph of a tumor section with hematoxylin/eosin (H/E) staining. Second, third, and fourth columns: MALDI-TOF-MS profile with detection of *BRAF*/*RAS* mutations. *X*-axis indicates mass-to-charge ratio (m/z) to distinguish wild-type and mutant allele, and Y-axis indicates signal intensity.

in 67% (23/34) of the 34 samples, whereas *HRAS*, *NRAS*, and *KRAS* mutations were detected less frequently, in 3% (1/34), 3% (1/34), and 0% (0/34) sample, respectively. Each oncogene mutation was mutually exclusive; 25 among the 34 samples (75%) were oncogene-mutation(+) cancer.

DNA METHYLATION ANALYSIS USING ILLUMINA INFINIUM BEADARRAY

Among 34 papillary thyroid cancer and 24 normal thyroid samples, 14 and 10 samples, respectively, were analyzed using Infinium 27K BeadArray. Methylation data of other cancer types (80 head and neck squamous cell cancers, 50 gastric cancers, 80 colorectal cancers, 80 prostate cancers, 24 chronic myeloid leukemias, 50 glioblastomas), and normal samples of corresponding tissues were collected from National Center for Biotechnology Information, Gene Expression Omnibus (http://www.ncbi.nlm.nih.gov/gds: GSE25089 for head and neck squamous cell carcinoma, GSE31789 for gastric cancer, GSE27130 for colorectal cancer, GSE26126 for prostate cancer, GSE31600 for chronic myeloid leukemia, and GSE22867 for glioblastoma). To analyze aberrantly methylated genes in cancer samples, probes with β-value < 0.17 in all the normal samples and with standard deviation of β-values in cancer samples >0.15 were selected, and shown in **Figure 2**. Each cancer type including papillary thyroid cancer showed a unique pattern of aberrant promoter methylation.

ABERRANTLY METHYLATED GENES IN PAPILLARY THYROID CANCER

While the number of aberrantly methylated genes was relatively small in papillary thyroid cancer (**Figure 2**), 25 genes showed frequent hypermethylation ($\beta > 0.25$) in three or more samples among the 14 papillary thyroid cancer samples, and no methylation ($\beta < 0.2$) in all the 10 normal samples (**Figure 3**). To check that the hypermethylation status was not due to contaminated blood cells, the methylation status of these genes in peripheral blood cells was also analyzed to see that none of them were methylated in blood (**Figure 3**).

Among 14 papillary cancer samples, 11 samples showed aberrant methylation in three or more genes, whereas the other three samples showed no aberrant methylation at all (**Figure 3**). When methylation status was compared with clinicopathological factors, the two cancer cases with recurrence were both methylation-negative ($P = 0.03$, Fisher's exact test) (**Figure 3**). Nine of the 11 frequently methylated samples showed mutation of *BRAF*/*RAS* oncogenes, whereas none of the three methylation-negative samples showed oncogene mutation ($P = 0.03$, Fisher's exact test). Other clinicopathological factors, including tumor size, lymph